PL-TR-91-2198

AURORAL-CLUTTER PREDICTIONS FOR FYLINGDALES, ENGLAND

Roland T. Tsunoda

SRI International
333 Ravenswood Avenue
Menlo Park, CA 94025

July 1991

Scientific Report No. 1

APPROVED FOR PUBLIC RELEASE; DISTRIBUTION UNLIMITED

PHILLIPS LABORATORY
AIR FORCE SYSTEMS COMMAND
HANSCOM AIR FORCE BASE, MASSACHUSETTS 01731-5000

"This technical report has been reviewed and is approved for publication"

EDWARD J. WEBER
Contract Manager

WILLIAM K. VICKERY
Branch Chief

FOR THE COMMANDER

ROBERT A. SKRIVANEK
Division Director

This report has been reviewed by the ESD Public Affairs Office (PA) and is releasable to the National Technical Information Service (NTIS).

Qualified requestors may obtain additional copies from the Defense Technical Information Center. all others should apply to the National Technical Information Service.

If your address has changed, or if you wish to be removed from the mailing list, or if the addressee is no longer employed by your organization, please notify GL/IMA, Hanscom AFB, MA 01731. This will assist us in maintaining a current mailing list.

Do not return copies of this report unless contractual obligations or notices on a specific document requires that it be returned.

REPORT DOCUMENTATION PAGE

Form Approved
OMB No. 0704-0188

1. AGENCY USE ONLY *(Leave Blank)*	2. REPORT DATE	3. REPORT TYPE AND DATES COVERED
	July 1991	Scientific No. 1

4. TITLE AND SUBTITLE
Auroral-Clutter Predictions for Fylingdales, England

5. FUNDING NUMBERS
F19628-90-K-0036
PE61102F
PR2310
TAG9
WUAJ

6. AUTHOR(S)
Roland T. Tsunoda

7. PERFORMING ORGANIZATION NAME(S) AND ADDRESS(ES)
SRI International
333 Ravenswood Avenue
Menlo Park, CA 94025

8. PERFORMING ORGANIZATION REPORT NUMBER
Interim Scientific Report,
SRI Project 1234

9. SPONSORING/MONITORING AGENCY NAME(S) AND ADDRESS(ES)
Phillips Laboratory
Hanscom Air Force Base, Massachusetts 01731-5000

Contract Manager: Edward J. Weber, /LIS

10. SPONSORING/MONITORING AGENCY REPORT NUMBER
PL-TR-91-2198

11. SUPPLEMENTARY NOTES

12a. DISTRIBUTION/AVAILABILITY STATEMENT
Approved for public release; distribution unlimited

12b. DISTRIBUTION CODE

13. ABSTRACT *(Maximum 200 words)*

Radar clutter produced by auroral processes in the ionospheric E layer, called auroral clutter, can have severe deleterious effects on surveillance radars that operate in the subauroral regions. Auroral clutter characteristics, however, are practically impossible to characterize with a statistical description because of the large number of controlling parameters. Recently, a predictive code called Comprehensive E-Region Auroral Clutter (CERAC) model has been written that uses knowledge of the underlying physics and semiempirical data as its basis. This report describes the predictions of the CERAC model for a surveillance radar located at Fylingdales, England. The results include predictions of occurrance, radar cross section, and Doppler velocity, all as functions of radar elevation, azimuth, range, and time.

14. SUBJECT TERMS
Radar clutter, auroral clutter, radar backscatter, ionospheric scatter, clutter prediction

15. NUMBER OF PAGES
30

16. PRICE CODE

17. SECURITY CLASSIFICATION OF REPORT	18. SECURITY CLASSIFICATION OF THIS PAGE	19. SECURITY CLASSIFICATION OF ABSTRACT	20. LIMITATION OF ABSTRACT
Unclassified	Unclassified	Unclassified	SAR

CONTENTS

ILLUSTRATIONS

I INTRODUCTION

A surveillance radar occasionally encounters clutter signals when scanning geographic sectors poleward of its site. These signals are called auroral clutter because of their known association with processes that produce the Aurora Borealis in polar regions. This class of radar clutter is confined to the E layer in the ionosphere, i.e., between 95 and 125 km altitude, but can have widespread geographic distribution. Auroral clutter can be a serious hinderance to radar performance because it is sometimes intense enough to affect radars that operate at frequencies as high as 3 GHz [e.g., *Chesnut et al.*, 1968]. Moreover, it is not confined to 'polar' regions as implied by its label but, in fact, can spread equatorward and appear at latitudes found in the northern continental United States. During highly-disturbed conditions, auroral manifestations have been detected over cities as low in latitude as Washington, D.C. Because the level of disturbance and frequency of occurrence are related to solar activity, auroral clutter poses a more serious problem in years of maximum solar activity than other times in the solar cycle.

Prediction of auroral clutter, in terms of occurrence in time and place and their characteristics when they do appear, has proven to be extremely difficult. It is virtually impossible to implement a statistical description of auroral-clutter characteristics because the number of controlling parameters is several and the amount of data required to adequately describe the joint statistics is beyond the scope of practicality. The most viable approach is to use our growing knowledge of the underlying physical processes and to combine the resulting theoretical predictions with existing statistical and empirical information on auroral clutter. This approach is more cost-effective than any attempt at large-scale accumulation of auroral-clutter data would be because ongoing research in the fields of plasma, auroral, and magnetospheric physics continues to make available new knowledge that can be applied to the auroral-clutter problem. Using this approach, a comprehensive E-region auroral-clutter (CERAC) model was developed by SRI International for the Rome Air Development Center [*Tsunoda et al.*, 1990].

The objective of the research effort described in this report was to use the CERAC model to predict auroral-clutter characteristics that would be observed by a surveillance radar located at Fylingdales, England. These predictions are described in this report together with a preliminary comparison to actual auroral-clutter observations made there.

II CERAC MODEL DESCRIPTION AND RESULTS

This section is divided into two parts: a brief description of the factors that control the occurrence and characteristics of auroral clutter, and model predictions of auroral-clutter characteristics for Fylingdales, England.

A. FACTORS CONTROLLING AURORAL CLUTTER

Three factors must be considered in order to make reasonable predictions about expected auroral-clutter characteristics:

- Magnetic aspect geometry
- Mean electron density in the E region
- The ionospheric electric field.

This information is needed for the radar scattering volume of interest. These factors, among others, are accounted for in the CERAC model and used in its predictions of auroral clutter. (See *Tsunoda et al.* [1990] for details of the CERAC model.)

1. Magnetic Aspect Geometry

The first factor in predicting auroral clutter, magnetic aspect geometry, determines the susceptibility of a radar at a specified site to auroral clutter. Auroral clutter is extremely aspect-sensitive; clutter strength is strongest when the radar beam orthogonally intersects the geomagnetic field ($\vec{B}$) and decreases rapidly as the angle with $\vec{B}$ deviates from 90°. The rate of decrease can be as rapid as 10 dB/deg. Because field-aligned irregularities in electron density that reside in the E region are responsible for auroral clutter, the magnetic aspect angle is important at those altitudes.

Figure 1 shows the magnetic aspect geometry for Fylingdales in polar coordinates centered on the radar site. (We have used the geographic and geomagnetic coordinates for York, England in lieu of Fylingdales coordinates. This approximate location makes

no essential difference to the model results.) The magnetic aspect angle, α, is defined as the angle made between the radar beam and the plane transverse to $\vec{B}$. The contours in Figure 1 represent loci of constant α at 110 km altitude. Similar contours can be determined for different altitudes in the E region; while similar in shape, they differ in detail. We have cross-hatched the region bounded by $\alpha = \pm 3°$ to indicate the most probable locations for auroral clutter that would be visible from Fylingdales if field- aligned irregularities that produce clutter are present. At the boundaries of this region, the clutter strength is expected to be about 30 dB weaker than would be seen along the $\alpha = 0°$ contour. All contours are shown arbitrarily to end at 1200 km ground distance, which is the nominal distance to the E layer for an elevation angle of 0° (if refractive effects are not important). Therefore, Figure 1 suggests that auroral clutter is not likely to be observed at azimuths west of $-290°$ nor at azimuths east of 60°. Between 320° and 20° azimuths, auroral clutter is likely to occur at ground distances between 280 and 420 km. It should be possible to detect auroral clutter at distances greater than 1200 km (where the contours close on themselves) only if propagation is supported by tropospheric refraction.

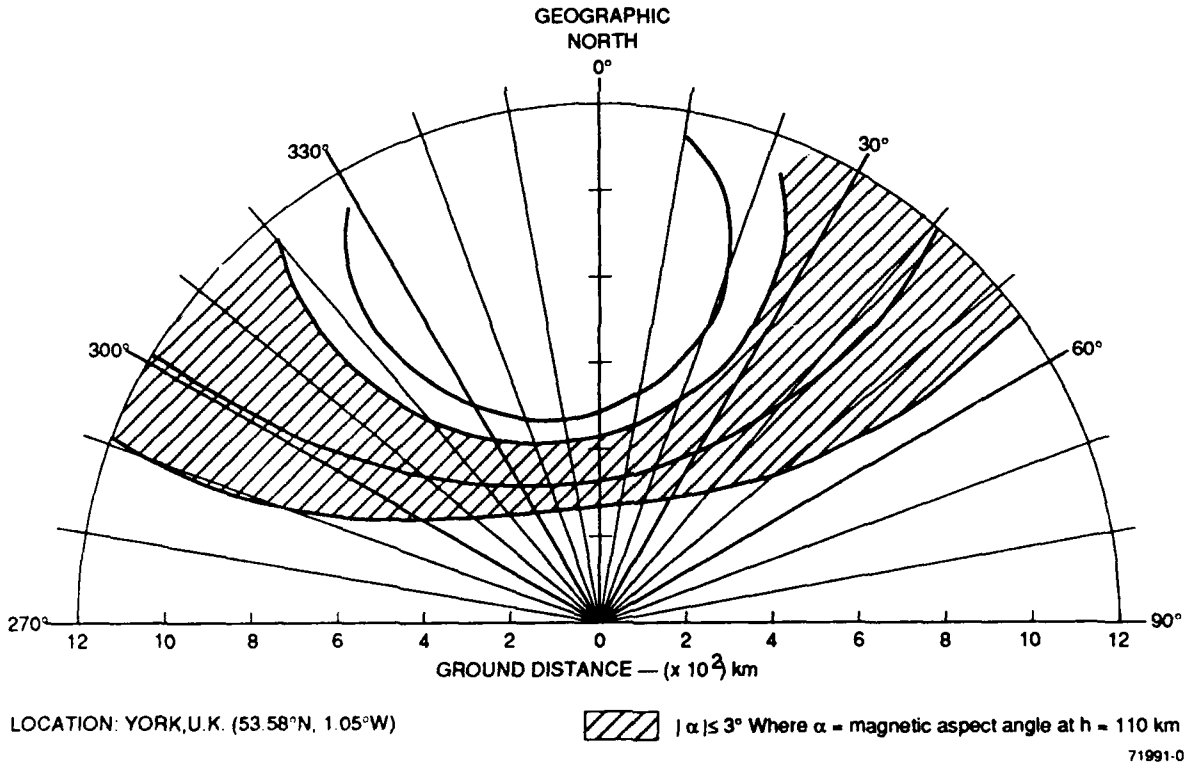

FIGURE 1 MAGNETIC-ASPECT GEOMETRY FOR FYLINGDALES, ENGLAND

2. Mean Electron Density

The second factor that needs to be considered when predicting auroral-clutter characteristics is the mean electron density in the E region. A minimum level of background ionization is needed because the irregularities responsible for auroral clutter are produced by fluctuations in electron density about a mean level. If the mean is zero, irregularities will not form. The sources of mean electron density in the E region are auroral particle precipitation and solar radiation during the day. While the solar-produced electron density is proportional to the solar zenith angle (i.e., the angle that the Sun's line of sight makes with the local vertical), that produced by auroral particles depends on where precipitation is occurring.

For our purposes, the precipitation region can be determined from the statistical location of the equatorward boundary of diffuse aurora determined by *Gussenhoven et al.* [1983]. Given this boundary, we can assume that the electron density is uniform poleward of that boundary. Structured electron densities associated with discrete precipitation usually exists poleward of the diffuse precipitation but can be ignored because they are beyond the Fylingdales' field of view. The equatorward boundary of diffuse precipitation is presented in Figure 2 as a function of geomagnetic latitude and geomagnetic local time. All five curves represent the same boundary whose location varies in latitude as a function of the local time and magnetic Kp index. This boundary is most poleward near noon and most equatorward around midnight. Although the boundary movement is equatorward with increasing Kp value, its rate of latitudinal descent is a function of local time.

We need to determine when auroral precipitation occurs in the field of view of the Fylingdales radar. That site is at a geomagnetic (eccentric dipole) latitude of 52.9°N. The contour labeled $\alpha = 3°$ in Figure 1 gets to the radar site is 280 km ground distance, which corresponds to 55.4°N. On the other hand, the point at 1200 km ground distance along the same meridian is at 63.7°N. Electron density produced by auroral precipitation, therefore, is likely to contribute in the midnight sector when $Kp > 2$ and in the dawn sector for $Kp > 3$. At other times, the Kp index must be higher for the boundary to reach the radar field of view. The latitudinal sector mentioned is not likely to receive auroral precipitation in the post-noon sector. This sector, therefore, relies on solar radiation for the needed ionization.

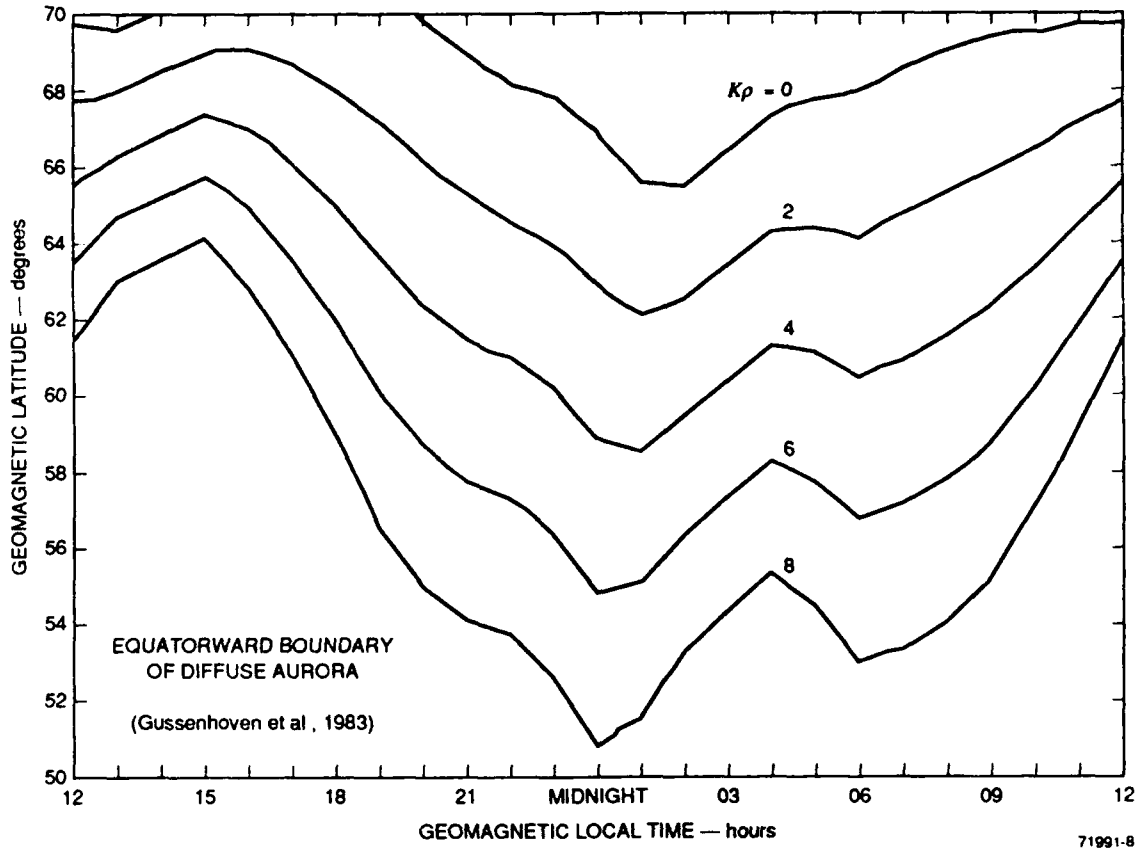

FIGURE 2 THE LOCATION OF THE EQUATORWARD BOUNDARY OF DIFFUSE AURORAL PRECIPITATION AS A FUNCTION OF THE MAGNETIC $K\rho$ INDEX

3. Ionospheric Electric Field

The third controlling factor in predicting auroral clutter is the ionospheric electric field, $\vec{E}$. Given the presence of significant electron density, the strength of $\vec{E}$ controls not only the generation of irregularities that produce auroral clutter but also the Doppler-velocity characteristics of the observed auroral clutter. Of the three factors, least is known about the behavior of $\vec{E}$. Without this knowledge, the occurrence or characteristics of auroral clutter cannot be accurately predicted. We have used the Heppner-Maynard (HM) $\vec{E}$ model [*Heppner and Maynard*, 1987] for the CERAC model calculations. It is an empirically constructed model that attempts to preserve most of the large-scale features in $\vec{E}$ that are measured *in situ* by satellites during any given traversal of the polar regions. In this sense, it is perhaps the most realistic of the available electric-field models. The HM $\vec{E}$ model is controlled by two parameters, the Kp index and the y-component (B_y) of the interplanetary magnetic field (IMF).

From the discussion above, it appears that the behavior of auroral-clutter characteristics can be described by two geophysical parameters, the Kp index and the B_y component of the IMF. The Kp index controls the equatorward extent of both auroral precipitation and the electric-field pattern and, therefore, plays the primary role. It is an index of global geomagnetic activity that is averaged over three-hour periods. These indices are published monthly with about a four-month delay in the *Journal of Geophysical Research.* (At present, near-real-time access to these indices is not possible. Because these indices are computed using magnetometer measurements from a number of observatories distributed globally, the speed of access depends on the availability of the measurements from all the observatories.) The B_y component of the IMF acts to distort and rotate the electric-field pattern. This behavior has relatively little effect on the equatorward extent of $\vec{E}$ and therefore should not significantly affect the occurrence of auroral clutter within a radar's field of view. However, the B_y effects can affect the Doppler velocity characteristics. The need for B_y is unfortunate because its value is not always measured experimentally and is not readily available when it is measured. (Measurements of the IMF requires a properly instrumented satellite to be situated outside the Earth's magnetosphere and preferably between the Sun and Earth. Such measurements are not made routinely and are not immediately available to the scientific community.)

Having placed the geophysical dependencies on Kp and B_y, it is natural to ask how they depend on solar activity and season. *Bartels* [1963] has shown that higher Kp values tend to occur more frequently during periods of high solar activity than during low activity. His results also indicate that there is a tendency for the highest Kp values to occur during the declining phase of a solar cycle. The seasonal dependence of the Kp index is known to maximize during the equinoxes [*Unger et al.*, 1973; *Tsunoda et al.*, 1990]. This semiannual dependence of Kp has been shown to be related to a similar dependence in the B_z component of the IMF and the solar wind speed [*Russell and McPherron*, 1973; *Maruyama*, 1974].

B. MODEL RESULTS

For the CERAC model runs, we assumed that the mean electron density has a fixed value of 10^5 el/cm^3. By making this assumption, the model output will represent nominal values that are independent of changes in the level of background ionization. This simplification is reasonable for this kind of investigation because electron densities produced by solar radiation and diffuse auroral precipitation are relatively uniform in spatial distribution and have comparable number densities. We also selected the $B_y > 0$ case for the HM $\vec{E}$ model because IMF data to determine B_y were not available. Al-

though this choice is arbitrary, it was not expected to impact predictions on the occurrence of auroral clutter.

For our 'most disturbed' case, we selected geomagnetic conditions specified by a Kp index of 7. As shown in Section III, these conditions are representative of periods when auroral clutter is present in the field of view from Fylingdales, but does not represent so disturbed a situation as to be considered a rarity in occurrence frequency. We also selected 1730 UT (universal time) for the time when spatial maps of auroral clutter would be computed with the CERAC model. (Because Fylingdales is located close to the Greenwich meridian, we assume throughout this report that UT approximates local time.) This time corresponds to the period of maximum clutter observations. For the Fylingdales radar parameters, we used an operating frequency of 435 MHz, a peak transmitted power of 1.2 MW, an effective pulsewidth of 1 μs, a circular (3 dB) beamwidth of 1.7°, and an antenna gain of 40 dB. The choice of pulsewidth is made to approximate radar performance. Because the clutter is assumed to be volume filling, radar performance using other pulsewidths can be scaled accordingly.

The CERAC model was run to simulate a sequence of azimuth scans at constant elevation angles. At each azimuth, auroral clutter strength (in dBm, i.e., received power referred to a milliwatt) and Doppler velocity (in m/s) were computed as a function of slant range, from 200 to 1500 km in 10-km range intervals. (Doppler velocity is used because it is independent of radar frequency. The Doppler frequency shift for the Fylingdales radar frequency of 435 MHz can be computed from the formula, $\triangle f = f \times v/150$, where $\triangle f$ is the Doppler shift in Hz, f is the radar frequency in MHz, and v is the Doppler velocity in m/s.) The clutter strength during azimuth scans at constant elevation angles (0° to 12.5° in steps of 2.5°) are presented in Figure 3. For each azimuth scan, auroral clutter appears as a band-like region extending in azimuth with a near-constant range. Each band is formed by backscatter that occurs as a function of altitude as the radar signal traverses the E layer. (The range extent of auroral clutter is *not* produced by the finite pulsewidth.) Because the scattering region has the form of a sheet of irregularities embedded at a fixed altitude, a band of auroral clutter moves closer in range when the elevation angle is increased. Each band narrows at the extreme azimuths because the conditions that control auroral clutter occurrence is altitude-dependent. The disappearance of auroral clutter at the extreme azimuths is controlled by the ionospheric electric field specified by the HM $\vec{E}$ model.

Within the bands, clutter strength is controlled by the magnetic aspect geometry. Auroral clutter, in this case, reaches power levels of –90 dBm at the extreme azimuths

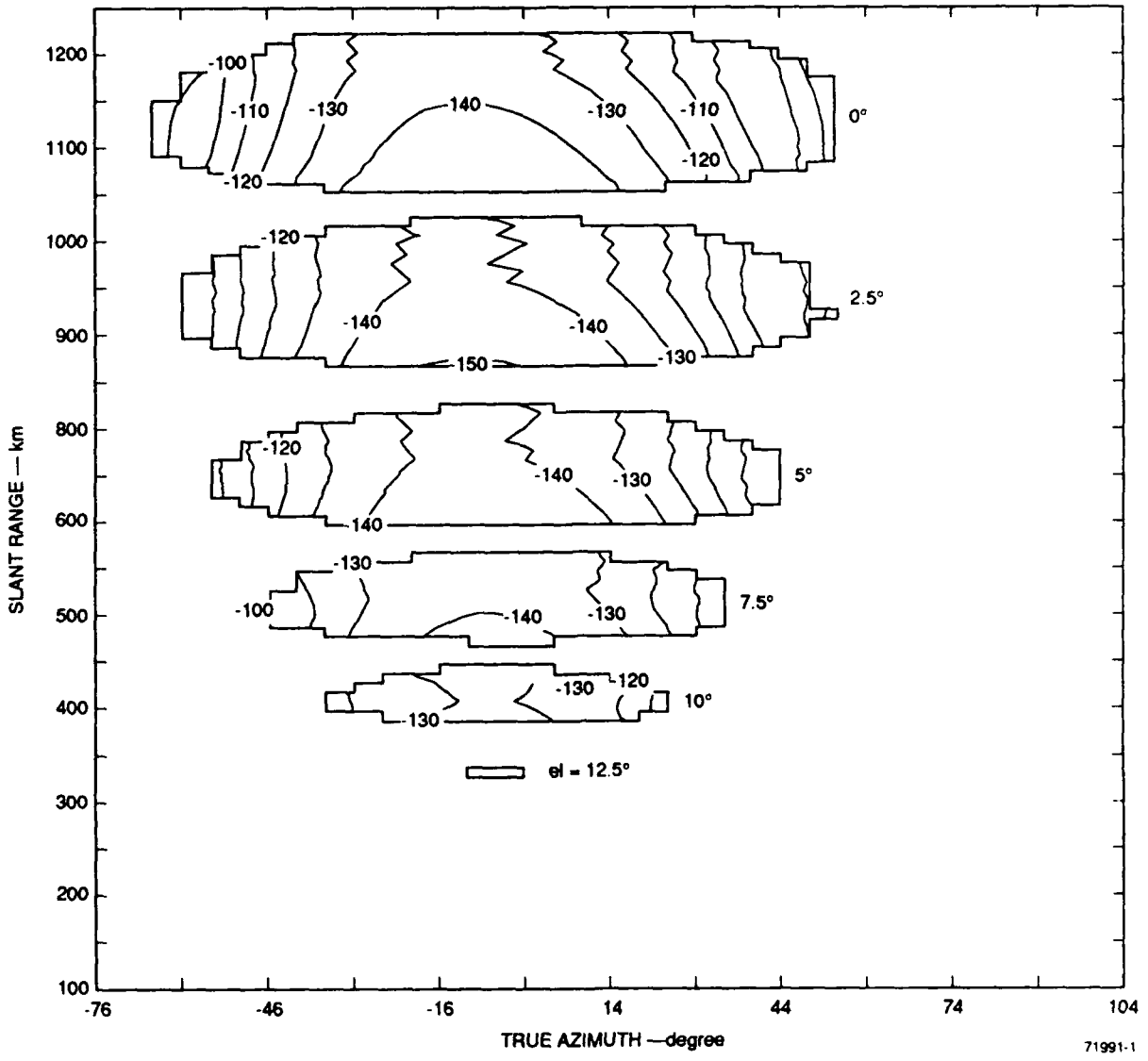

FIGURE 3 CONTOUR PLOTS OF AURORAL-CLUTTER STRENGTH (dBm) AS A FUNCTION OF SLANT RANGE AND TRUE AZIMUTH, FOR $K\rho = 7$

The six regions describe the auroral clutter obtained at fixed elevation angles, from 0° to 12.5° in steps of 2.5°

at zero elevation angle and decreases by as much as 50 dB toward the center of the scan. This pattern can be inferred from the magnetic aspect contours shown in Figure 1. (Note that system sensitivity or noise level is not considered in this computation.) The appearance that clutter strength cuts off abruptly is an artifact of the CERAC model. The reason is that occurrence of clutter is determined by a threshold condition while clutter strength is determined from an empirical relationship that is independent of the electric field strength. In reality, other processes would enter to smooth the transition

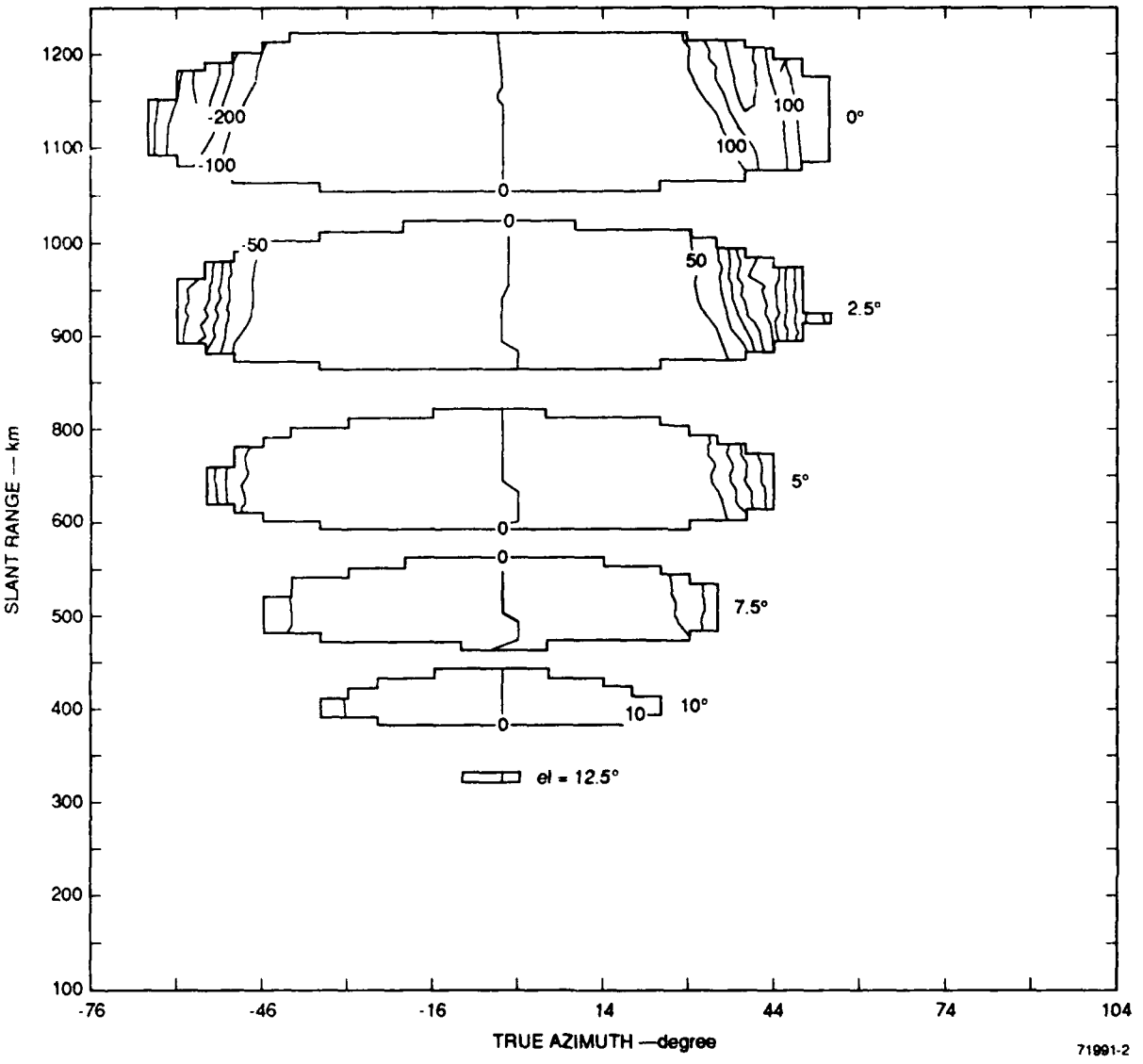

FIGURE 4 CONTOUR PLOTS OF DOPPLER VELOCITY (m/s) THAT CORRESPOND TO THE AURORAL-CLUTTER REGIONS IN FIGURE 3 ($K\rho$ = 7 case)

out as expected from nature. These processes have not been included in this model.

Figure 4 shows contour plots of Doppler velocity that correspond to the clutter-strength plots in Figure 3. The zero-Doppler crossovers from negative Doppler velocities at west azimuths to positive Doppler velocities at east azimuths are seen as near-vertical lines at an azimuth close to zero. There is a latitudinal gradient in Doppler velocity that may not be immediately evident because different velocity intervals have been used for the contours at different elevation angles. For example, at zero elevation, the contours

are plotted at 100-m/s intervals. At 2.5°, the contour intervals are 50 m/s. Comparing the azimuths of the 100-m/s contours in these two bands, we find that those at zero elevation are closer to the zero Doppler crossover than those from 2.5° implying that the velocities are higher at farther ranges. The contour intervals in the 5° elevation band is also 50 m/s while those in the 7.5° band are 20 m/s. The last two bands have contour intervals of 10 m/s.

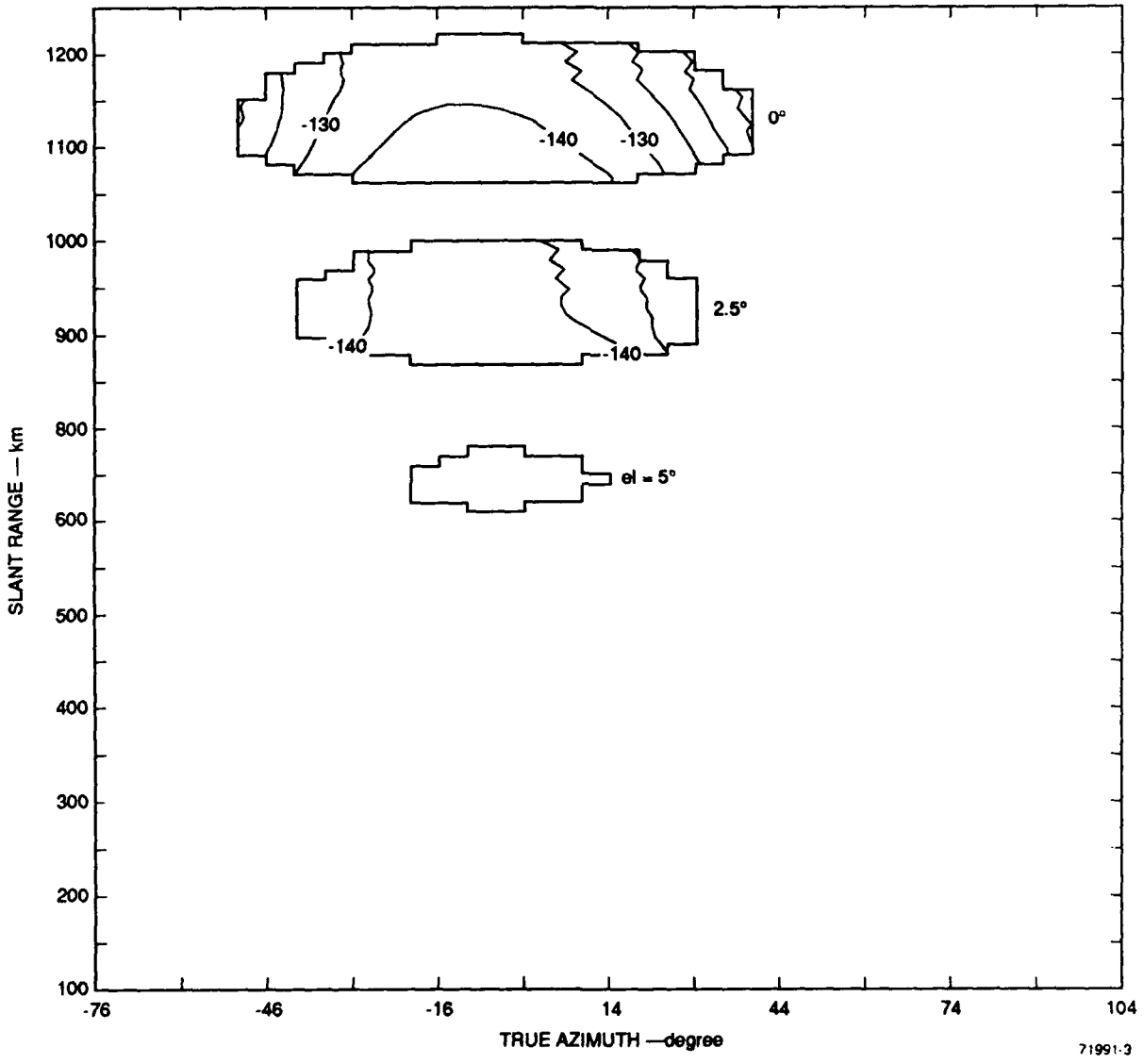

FIGURE 5 CONTOUR PLOTS OF AURORAL-CLUTTER STRENGTH SIMILAR TO THOSE IN FIGURE 3 BUT FOR $K\rho = 6$

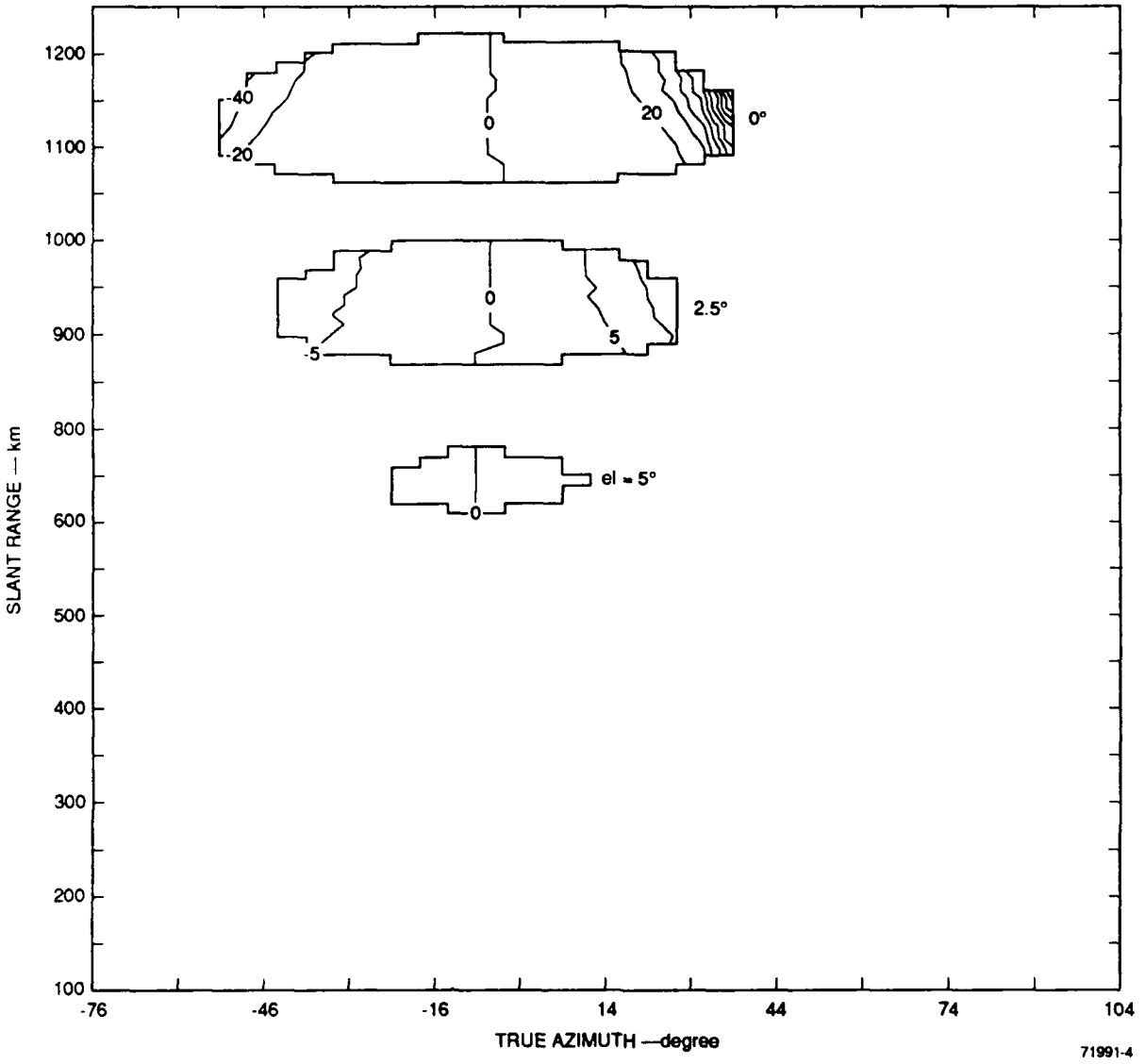

FIGURE 6 CONTOUR PLOTS OF DOPPLER VELOCITY THAT CORRESPOND TO THE AURORAL-CLUTTER REGIONS IN FIGURE 5 (Kp = 6 case)

Figures 5 and 6 are results from a 'less disturbed' case, specified by $Kp = 6$. The bands of clutter strength in Figure 5 differ from those in Figure 3 in number and size. The closer bands are absent, indicating that the region containing ionospheric irregularities (that produce auroral clutter) did not extend as low in latitude as the $Kp = 7$ case. The other difference is that, for the same elevation angle, the size of each band is smaller in the less-disturbed case. The Doppler velocities associated with this set of auroral clutter results, presented in Figure 6, are somewhat smaller than those in Figure 4, indicating weaker electric fields. The CERAC model was also run for the cases, $Kp = 4$ and

5. Figures to illustrate those results are not presented because the qualitative features are similar. No auroral clutter was detected for the $Kp = 4$ case; for the $Kp = 5$ case, a band smaller in size than shown in Figure 5 was obtained for 0° elevation, but none was obtained for elevation angles of 2.5° and above. A small band of auroral clutter was obtained at 1.5° elevation.

From this set of results, we conclude that auroral clutter is predicted by the CERAC model to be visible within the field of view of the Fylingdales radar for conditions specified by Kp values greater than 4. If the lowest elevation angle used is 2.5° (an elevation angle used to collect the Fylingdales clutter data, see Section III), auroral clutter will not be visible unless Kp is greater than 5. Therefore, the CERAC model predicts a threshold in Kp index value of 5 for the occurrence of auroral clutter in the radar field of view. The threshold Kp value derived from the above model runs applies only to this time period. In other words, the occurrence of auroral clutter also has a local time dependence.

To represent the local time variation of auroral-clutter occurrence, we again selected the $Kp = 7$ case. This time, the CERAC model was run at hourly intervals in UT for the complete 24-hour period, using a fixed azimuth of 355° (assumed to be near the magnetic meridian) and a fixed elevation of 2.5°. The results are presented in Figure 7. Auroral clutter strength is plotted as a function of slant range for each hourly interval that clutter is predicted. Auroral clutter is not predicted for this antenna position between 0900 and 1500 UT, i.e., ±3 hours about local noon. At 1600 UT, the range extent predicted is nearly as wide as those between 1700 and 2000 UT, which suggests that the electric field did not increase slowly but that its pattern moved into the radar field of view at this time. Between 2100 and 2200 UT, we see a behavior produced by a spatially varying electric-field pattern (a region called the Harang discontinuity). Auroral clutter strength returns to full strength at 2300 UT and maintains its strength through midnight. Thereafter, the extent of auroral clutter decreases slowly, indicating a corresponding weakening of the electric field with time.

From Figure 7, we draw the following conclusions. Auroral clutter is predicted to be absent at 2.5° elevation between 0900 and 1500 UT for a Kp index of 7, our most disturbed case. The threshold Kp value for clutter detection is likely to be higher than 5 for times around 2100 and 2200 UT, and also around the morning hours.

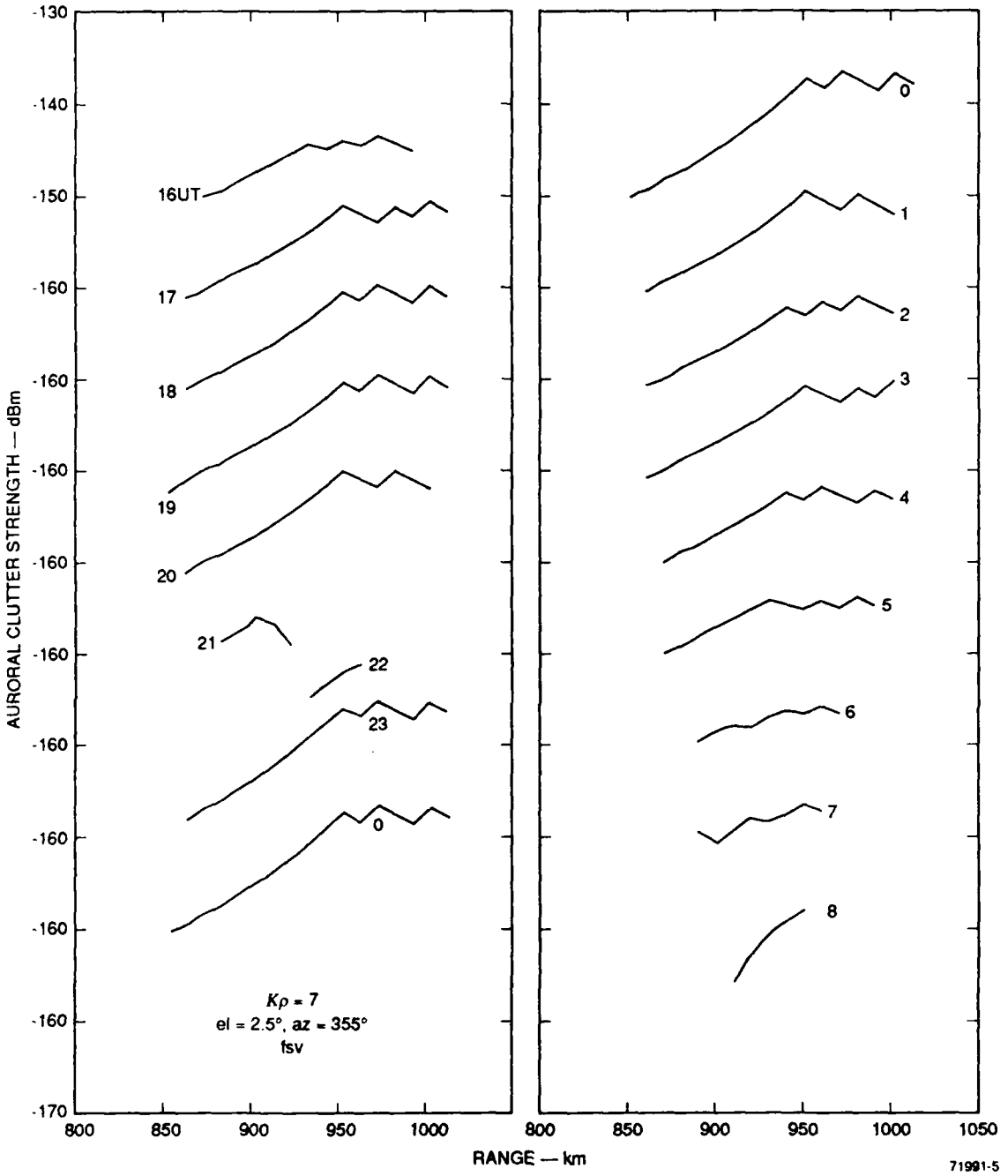

FIGURE 7 STACKED PLOTS OF AURORAL-CLUTTER STRENGTH AS A FUNCTION OF SLANT RANGE, $K\rho = 7$

Plots are shown for hourly intervals; auroral clutter was not seen for four hour intervals that are not shown

C. SUMMARY OF MODEL PREDICTIONS

For the Fylingdales radar site, we can make the following predictions regarding auroral clutter on the basis of the current CERAC model:

- During the course of a day, auroral clutter is most likely from 1700 to 1900 UT, and 2300 to 0300 UT (see Figure 7). Conversely, clutter occurrence is not expected at all during the period ±3 hours about local noon.

- At 1730 UT, auroral clutter should occur whenever the magnetic Kp index is greater than 4. This prediction should hold more or less for the periods given in prediction 1. At other times, the threshold Kp value must be higher than 5.

- When auroral clutter is present, it is most likely to be observed to the north in the azimuth sector bounded by 290° and 60°. The azimuthal extent is dependent on elevation angle.

- When the radar is scanned in azimuth at a fixed elevation angle, the envelope of the auroral-clutter appears as a band-like region that extends in azimuth, but located at a near-constant range.

- While the envelope has a band-like shape, the distribution in the strength of auroral clutter will resemble that shown in Figure 1. In most cases, clutter strength will maximize at extreme east and west azimuths.

- The Doppler velocities can be expected to vary with azimuth and have speeds up to ±300 m/s around 1730 UT. The Doppler velocities can be much higher (up to 800 m/s) at other times. (This model result was not demonstrated as part of this investigation.) At 435 MHz, 300 m/s corresponds to 870 Hz.

- The dependence of auroral-clutter occurrence on the magnetic Kp index implies the following: Clutter occurrence should maximize semiannually around the equinoxes, and also during solar maximum years and those years during the declining phase of the solar cycle. (The exact behavior of the Kp index during the declining phase of the solar cycle is not clear. Its statistical behavior remains to be quantified.)

III COMPARISON OF MODEL RESULTS TO MEASUREMENTS

A. FYLINGDALES DATA

Auroral-clutter observations from Fylingdales have been reported in terms of start and stop times for each event and with sample tracings of auroral-clutter regions as functions of azimuth and slant range. For this investigation, we have analyzed 23 such events detected between May and September 1990. The dates and times of these events are listed in Table 1 together with magnetic Kp indices that correspond with all three-hour periods during which auroral clutter was observed. We use these indices to classify the events for comparison with the CERAC model results presented above. Before proceeding, we note that because the parameters of the old Fylingdales radar were not available for this investigation, comparisons are made between model results computed using the new radar parameters and observations made with the old radar parameters. Discrepancies between model results and observations that may be produced by the differences in radar parameters are noted during discussion.

Figure 8 shows the times of the 23 auroral-clutter events. Their durations range from 20 minutes to 17 hours. Clutter observations were detected most in the dusk sector while none were detected during late morning. This distribution is clearly seen in Figure 9 where we present a histogram of these occurrences in 3-hour blocks (to facilitate classification by the Kp index). The largest number of events were seen between 1500 and 1800 UT, i.e., the late afternoon period. The maximum in occurrence is followed by a gradual decrease until about 0300 UT. The decrease is more rapid thereafter until no events were observed between 0900 and 1200 UT.

The histogram is in reasonable agreement with the predictions of the CERAC model. The occurrence maximum between 1500 and 1800 UT resembles one of the maxima predicted by the model from 1700 to 1900 UT. The apparent time displacement of the observed maximum to earlier times might be attributed to a B_y effect, which we have not accounted for. This discrepancy may, in fact, be more serious. The observation of six events between 1200 and 1500 UT is not predicted at all by the CERAC model. These events, combined with the apparent displacement of the occurrence maximum, suggest a feature that may be geophysically significant. Further discussion is presented

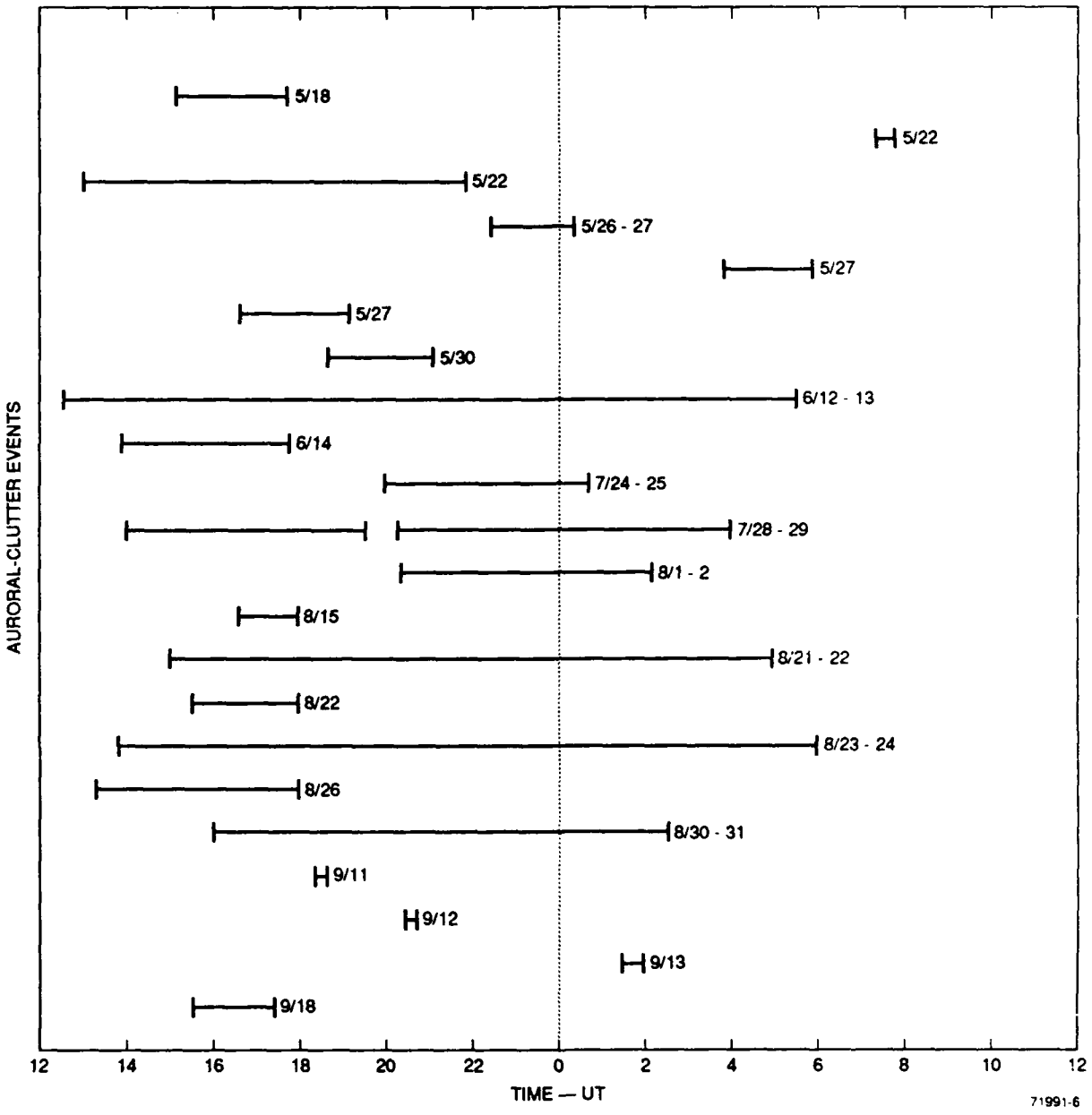

FIGURE 8 BAR GRAPH SHOWING THE PERIODS WHEN AURORAL CLUTTER WAS OBSERVED, FROM MAY 18 TO SEPTEMBER 18, 1990

in Section IV. The predicted lull in clutter activity between 2000 and 2200 UT is not apparent in Figure 9. However, the disagreement is not severe in that auroral clutter occurrence during this period (although weaker) is predicted by the CERAC model. The rapid decrease in auroral-clutter events after 0300 UT and a cutoff beyond 0900 UT is, however, in excellent agreement with the CERAC model.

Table 1
Fylingdales Auroral-Clutter Observations
May – September 1990

Event	Date (UT)	Time (UT)	*Kp* Index
1	5/18	1510 to 1743	6+
2	5/22	0720 to 0750	5+
3	5/22	1300 to 2150	5, 4, 4–, 3+
4	5/26-27	2224 to 0022	7+, 4–
5	5/27	0350 to 0550	6+
6	5/27	1640 to 1910	4+, 3–
7	5/30	1840 to 2104	5
8	6/12-13	1230 to 0533	5+, 7, 8–, 8+, 8–, 6
9	6/14	1350 to 1745	7+, 8–
10	7/24-25	2000 to 0040	1+, 0+, 1
11	7/28	1400 to 1930	7–, 7+, 8–
12	7/28-29	2015 to 0400	8–, 8–, 7, 7
13	8/1-2	2020 to 0210	5, 5–, 3+
14	8/15	1635 to 1800	5–
15	8/21-22	1500 to 0500	6–, 6, 5, 5+, 6–
16	8/22	1525 to 1800	4+
17	8/23-24	1345 to 0600	7, 6+, 6+, 4+, 4, 5+
18	8/26	1340 to 1800	7–, 6
19	8/30-31	1600 to 0234	5+, 4–, 4–, 5–
20	9/11	1820 to 1840	4
21	9/12	2030 to 2040	4–
22	9/13	0130 to 0200	5–
23	9/18	1530 to 1720	4

To further characterize our 23 events, we have plotted the 3-hour occurrences as a function of the magnetic *Kp* index in Figure 10. The histogram reveals a striking dependence of auroral-clutter occurrence on the *Kp* index. Virtually all of the auroral-clutter events occurred during periods when *Kp* was 4– or greater. There was one occurrence when *Kp* was 0, two when *Kp* was 1, and three when *Kp* was 3. In contrast, there were 50 3-hour periods when *Kp* was greater than 4–. If we remove the four events that lasted less than an hour, the distribution changes little, as shown by the dashed lines. The observed threshold for auroral-clutter occurrence is in good agreement with the

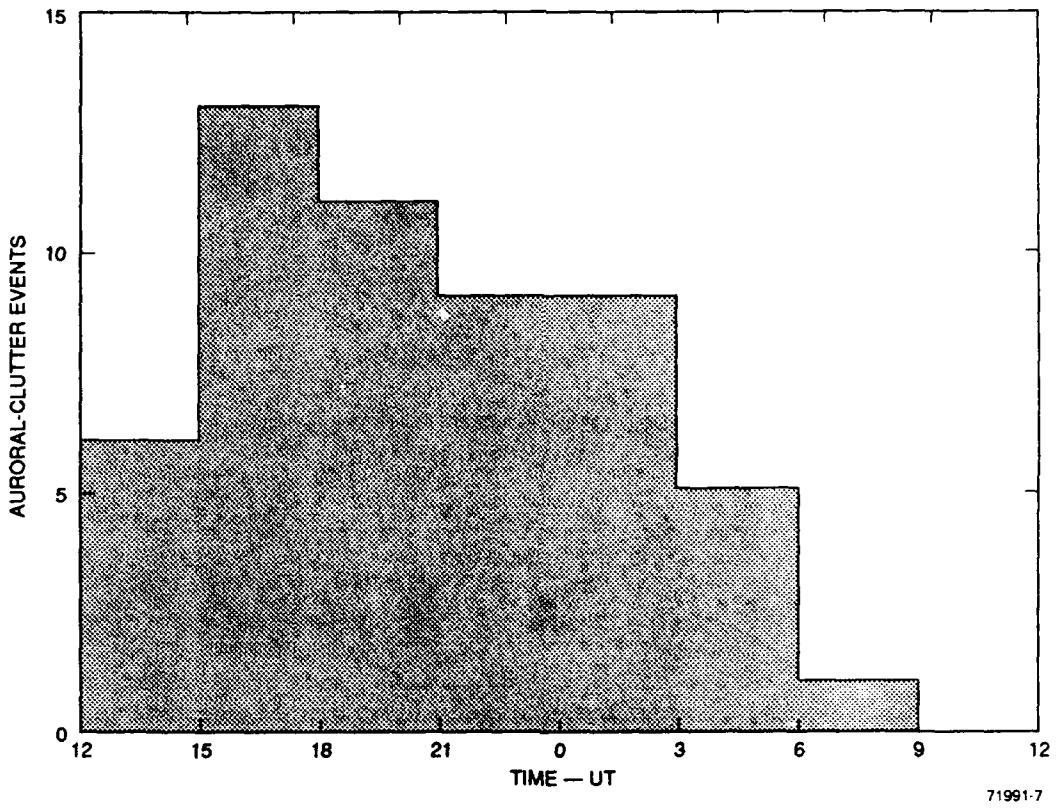

FIGURE 9 HISTOGRAM OF THREE-HOUR AURORAL-CLUTTER EVENTS AS A FUNCTION OF UT

predicted Kp threshold value of 4. We should note that the predicted threshold for the Kp index is for a radar elevation angle of 0° while all of the radar observations are believed to be made with an elevation angle of 2.5°. If this higher elevation angle is used, the predicted threshold in Kp index increases to 5. However, we consider the prediction to be in good agreement with observations because the old radar beamwidth was much larger than the new beamwidth used. A broader beamwidth would allow detection of auroral clutter at lower elevation angles. This threshold Kp value is likely to hold at least for the most probable periods, 1700 to 1900 UT, and 2300 to 0300 UT. The occurrence of auroral clutter during three 3-hour periods when the Kp index was less than 2 is curious. While they did occur during the midnight sector (see Table 1) when auroral clutter is most probable, the Kp values are much lower than the predicted threshold value.

To evaluate the statistical validity of this threshold in Kp index for auroral-clutter occurrence, we can compare the distribution in Figure 10 to various statistical distributions of Kp-index values. In Figure 11, we have plotted (solid-line curve) the statistical distribution of all Kp indices from 1932 to 1971 [*Cage and Zawalick*, 1972]. Superimposed on this curve is a plot (dashed-line curve) of the relative occurrence of Kp values

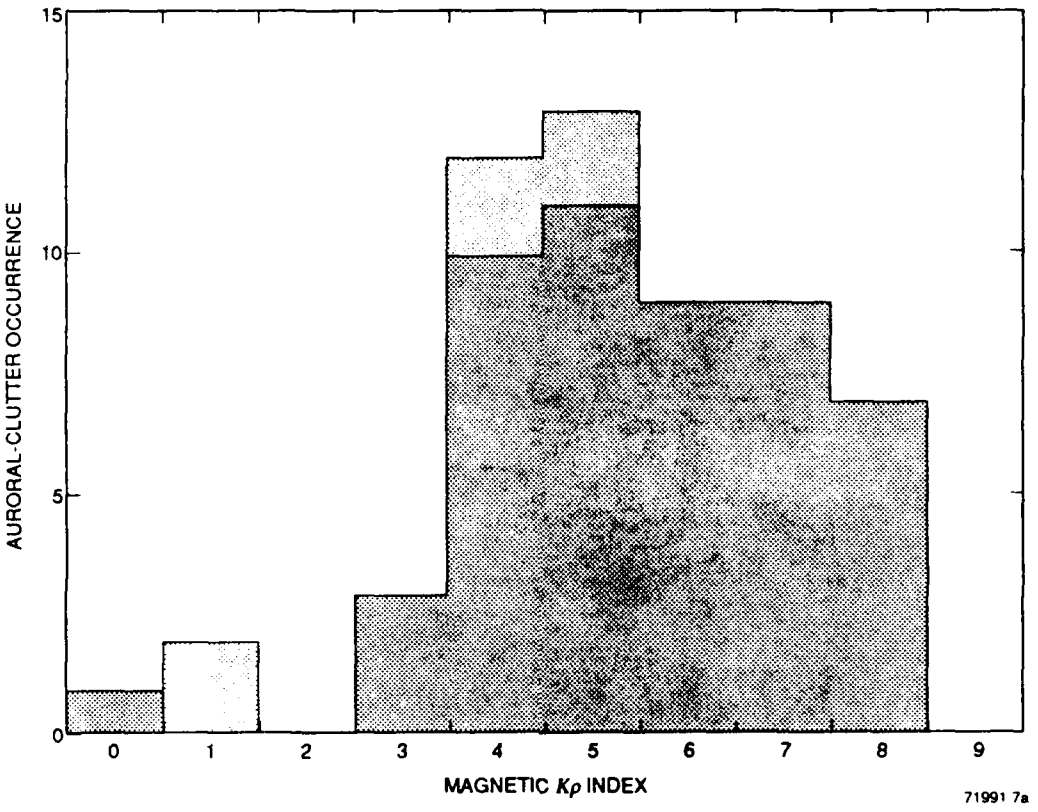

FIGURE 10 HISTOGRAM OF THREE-HOUR AURORAL-CLUTTER EVENTS AS A FUNCTION OF THE MAGNETIC Kp INDEX

from June through August 1990. (The occurrence frequencies for the individual months are also plotted using the three symbols.) Both curves are similar, showing a broad maximum in occurrence frequency between 1 and 3 followed by a rapid decline at higher Kp values. These distributions indicate that geomagnetic activity during the three months were not unusual (while suggestive of slightly higher activity than the statistical mean). When compared to the histogram in Figure 10, we find that the auroral-clutter events are not common by any means and that the Kp threshold value suggests a deterministic behavior. Conceptually, we can integrate the curves in Figure 11 to derive quantitative estimates for the probability of occurrence.

B. AURORAL-CLUTTER TRACINGS

Each tracing of auroral-clutter regions found in the clutter reports was made from a Fylingdales radar scan that presumably consisted of an azimuth scan at a constant elevation of 2.5°. The azimuth scans were one of two: from 284° to 14° with a center azimuth of 329°, and from 14° to 104° with a center azimuth of 59°. In most cases, the

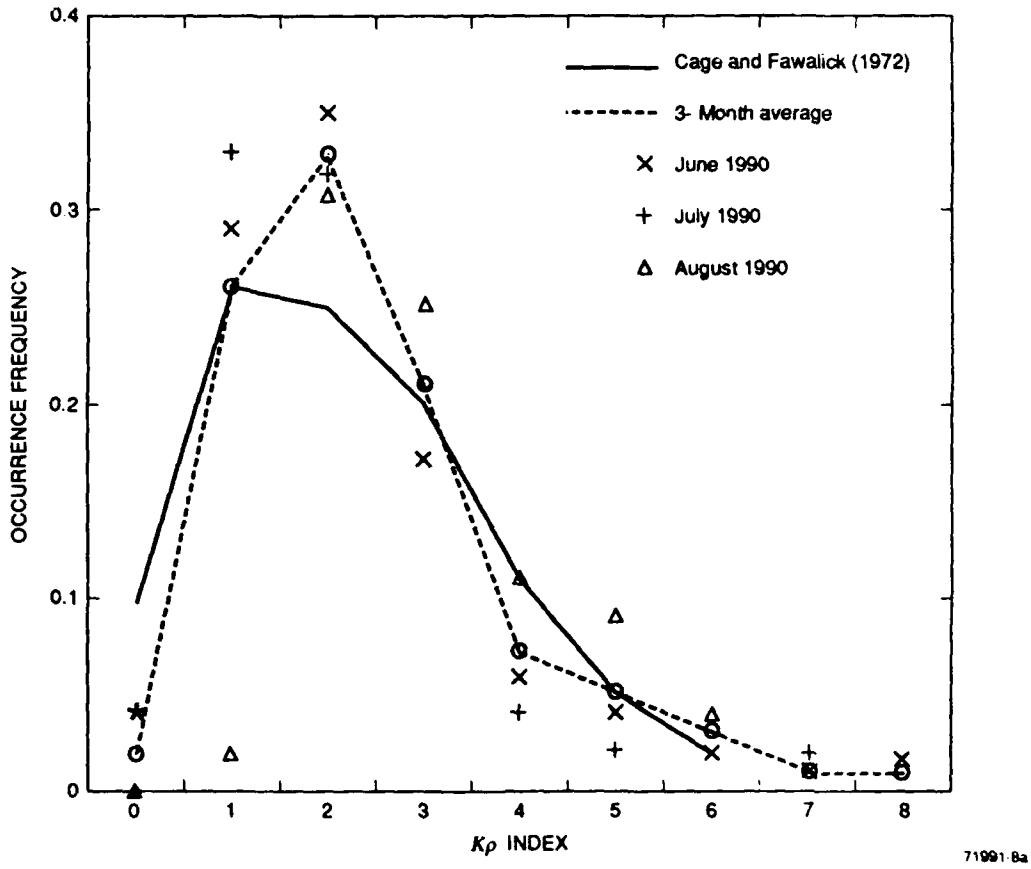

FIGURE 11 THE OCCURRENCE FREQUENCY OF MAGNETIC Kp INDICES FOR MONTHS OF JUNE, JULY AND AUGUST 1990, THEIR THREE-MONTH AVERAGE, AND COMPARISON TO THE AVERAGE CURVE FOR YEARS 1932 TO 1971 (Cage and Zawalick, 1972)

tracings were presented as two halves of a selected azimuth scan. Representative examples are described below.

The clutter map presented in Figure 12 was taken on 27 May 1990 around 1715 UT, when the magnetic Kp index was 4+. The two halves of the scan have been spliced together at 14° true azimuth. The discontinuity in the traced lines suggests temporal variability during the two scans. (To our knowledge, the fact that the left half of the scan is cross-hatched and the right half is not has no quantitative significance.) Slant range is given in nautical miles, which can be converted to kilometers by multiplying by 1.852. Therefore, 300 nm corresponds to 556 km, 600 nm to 1111 km, and 900 nm to 1667 km. The clutter region appears as a band extending in azimuth from 288° on the west side to about 60° on the east side. Small patches of clutter are to be seen out to nearly 100°. This clutter band appears at near constant ranges, from about 360 nm (667 km) to almost 800 nm (1482 km).

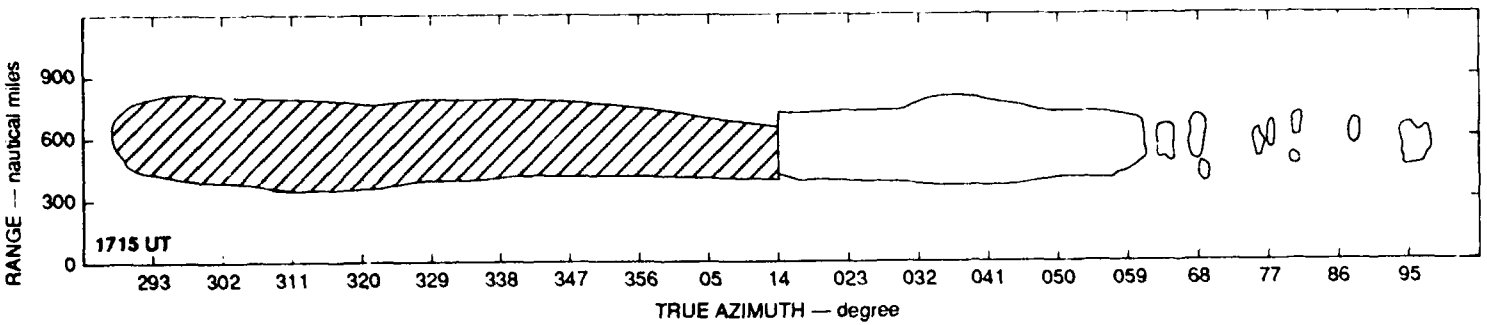

FIGURE 12 AURORAL-CLUTTER TRACINGS, 1715 UT, 27 MAY 1990
Slant range is given in nautical miles.

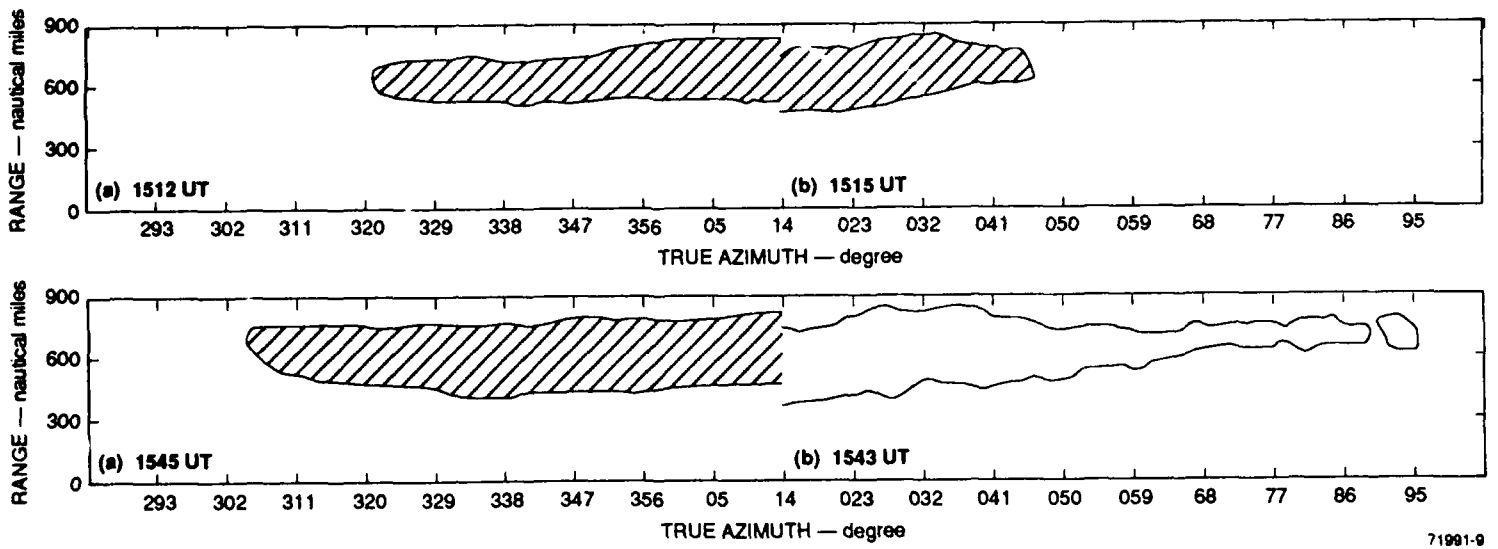

FIGURE 13 AURORAL-CLUTTER TRACINGS, 1512 TO 1543 UT, 18 MAY 1990

A second set of clutter maps is presented in Figure 13. The measurements were made between 1500 and 1600 UT on 18 May 1990 when the Kp index was 6+. The clutter regions again appear as banded regions with near constant ranges. They closely resemble that in Figure 12 except those in Figure 13 are less extended in azimuth. The range extent of the auroral clutter in the lower map narrows at the east azimuths, suggesting that the patches in Figure 12 are probably part of the band but perhaps weaker and therefore patchy in appearance.

Figure 14 is a third set of clutter maps taken over a longer time period. These measurements were made from 1300 to 2000 UT on 22 May 1990 when the Kp indices were 5, 4, and 4–. The auroral clutter region is most variable in azimuth. The region is narrowest around 1300 UT, expanding to maximum extent around 1730 UT, then breaking up into two distinct east and west regions at later times.

The patterns of auroral-clutter strength presented in Figure 3 can be compared to the auroral-clutter tracing in Figure 12. The tracing extends in slant range from 400 nm (741 km) to 800 nm (1482 km) with its center located about 600 nm (1111 km). Therefore, this tracing appears to encompass slant ranges from the center of the azimuth scan at 5° elevation to perhaps 250 km beyond the model clutter band from an azimuth scan at 0° elevation. This overlap is consistent with the old Fylingdales radar beamwidth being about three times wider than that used in the CERAC model runs. The displacement of the tracing in range to farther ranges than predicted by the model could simply be because neither tropospheric nor ionospheric refraction corrections have been implemented in the CERAC model. Such refractive effects could account for the range displacement.

The tracing in Figure 12 extends from −72° to 60° true azimuth which compares favorably with the azimuth extent of the model results for an elevation angle of 0°. The clutter region in Figure 13 extends from −68° to 54°. The auroral clutter seen at east azimuths greater than 60°, as shown in Figures 12 and 13 (but not Figure 14), is not predicted by the CERAC model. These echoes would require another clutter mechanism.

The model predictions in Figure 3 are also consistent with the tracings presented in Figure 14. In this event, the auroral-clutter region appears as two patches, one centered around 300° (−60°) azimuth and the other around 40° azimuth. These patches are seen to be located at azimuths where the clutter strength is strongest in the model run at zero elevation, in Figure 3. Because clutter strength varies over 50 dB, the central portion of that band could be below the sensitivity threshold of the radar on this occasion.

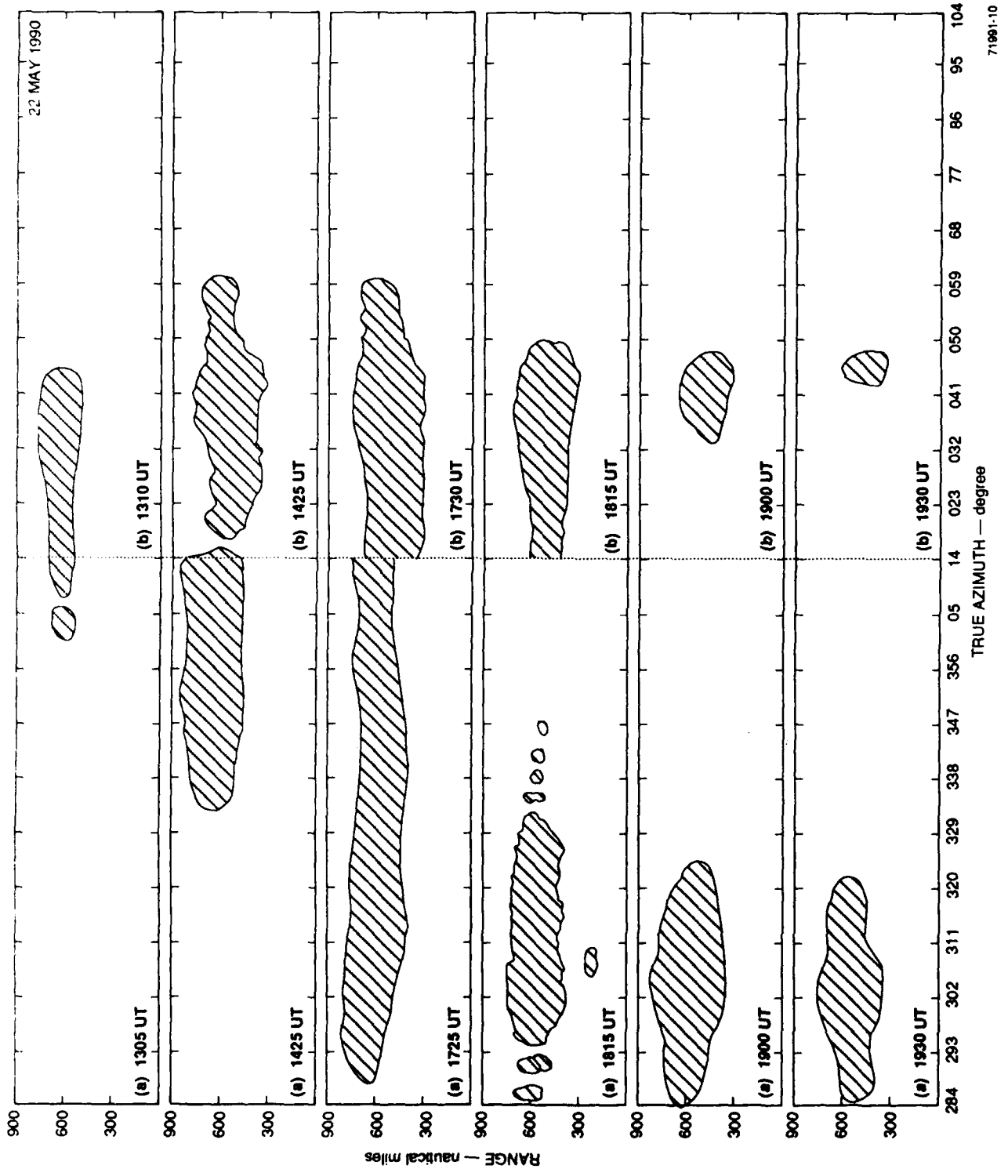

FIGURE 14 AURORAL-CLUTTER TRACINGS, 1305 TO 1930 UT, 22 MAY 1990

C. SUMMARY OF COMPARISONS

Conclusions drawn from the comparisons of model predictions with data are as follows:

- The observed occurrence frequency of auroral clutter as a function of local time is in reasonable agreement with model prediction. The maximum in the dusk to early evening period and the post-midnight decline in clutter activity are seen in observations and model results.

- The occurrence of auroral clutter in the early post-noon sector is not predicted. A predicted lull in clutter activity around 2100 UT is not seen in observations.

- The threshold Kp index of 4 is in excellent agreement with observations. Presumably, higher threshold values predicted for different local times would be masked in a histogram such as shown in Figure 10.

- The CERAC model does not predict occurrence of auroral clutter in the midnight sector when the Kp index was less than 2.

- The azimuthal sector in which auroral clutter is observed is in good agreement with model predictions. Auroral clutter sometimes seen at more easterly azimuths is not predicted by the model.

- The azimuthal distribution in the strength of auroral clutter is in good agreement with model predictions, which are controlled primarily by the magnetic aspect geometry.

- Absolute clutter strength and associated Doppler velocity associated with observations were not available and therefore could not be compared to predictions by the CERAC model.

IV DISCUSSION AND RECOMMENDATIONS

We have shown that the CERAC model is capable of predicting auroral clutter with reasonable accuracy. Both model prediction and observations have revealed a strong dependence of auroral-clutter occurrence on the magnetic Kp index. Given this strong dependence on the Kp index and the availability of these indices from 1932 to 1971 (e.g., used by *Cage and Zawalick* [1972] and *Maruyama* [1974]), it is now possible to quantify these model predictions in a more statistical manner. That is, the probabilities of occurrence for all Kp values can be computed as a function of season and solar activity. These probabilities can then be used to predict the probabilities of auroral-clutter occurrences. Quantification in this manner should be useful to the radar operator.

Several improvements to the CERAC model are recommended. If there is concern for more accurate estimates on the spatial distribution of auroral clutter, tropospheric refraction effects should be implemented. This correction becomes important at low elevation angles. If a need exists to estimate the clutter strength accurately, a more realistic algorithm for electron density should be implemented. If a need exists for accurate Doppler velocity estimates, electron heating effects should be implemented. Finally, if there is interest in developing a scheme for predicting auroral clutter that is more realistic than a Kp index dependence, we recommend using auroral-particle and electric-field measurements by the Air Force DMSP satellites to make near-real-time predictions.

A few unexpected differences were also found between model results and observations. The occurrence of auroral clutter in the midnight sector when low Kp values were recorded is not predicted and requires investigation. The occurrence of clutter events in the early post-noon sector fall into the same category. Both types of events suggest the presence of unexpected substantial electric fields and electron densities in the subauroral region. Measurements have been made of large electric fields in the subauroral zone during the dusk sector; however, it is not known to what extent such fields penetrate into the afternoon sector. These discrepancies are important because radars (such as that at Fylingdales) that view the subauroral region would encounter auroral-clutter events not predicted by the CERAC model. We therefore strongly recommend this investigation if more accurate model predictions are desired.

REFERENCES

Bartels, J.,1963: "Discussion of the Time-Variations of Geomagnetic Activity, Indices *Kp* and *Ap*," *Ann. Geophys.*, Vol. 19, No. 1, pp. 1-20.

Cage, A.L., and E.J. Zawalick, 1972: "A Discussion of the Geomagnetic Indices *Kp* and *ap*, 1932 to 1971," AFCRL-72-0693 (AD756828), Air Force Cambridge Research Laboratories, L.G. Hanscom Field, Bedford, Massachusetts.

Chesnut, W.G., J.C. Hodges, and R.L. Leadabrand, 1968: "Auroral Backscatter Wavelength Dependence Studies," Final Report, Contract AF 30(602)-3734, Stanford Research Institute, Menlo Park, California.

Gussenhoven, M.S., D.A. Hardy, and N. Heinemann, 1983: "Systematics of the Equatorward Diffuse Auroral Boundary, *J. Geophys. Res.*, Vol. 88, p. 5692.

Heppner, J.P., and N.C. Maynard, 1987: "Empirical High-Latitude Electric Field Models," *J. Geophys. Res.*, Vol. 92, p. 4467.

Maruyama, T., 1974: "Origin of the Semiannual Variation of Geomagnetic *Kp* Indices," *J. Geophys. Res.*, Vol. 79, p. 297.

Russell, C.T., and R.L. McPherron, 1973: "Semiannual Variation of Geomagnetic Activity," *J. Geophys. Res.*, Vol. 78, p. 92.

Tsunoda, R.T., M.F. Williams, and Y. Zambre, 1990: "A Comprehensive *E*-Region Auroral Clutter (CERAC) Model, Volume 1 – Description, Results, and Validation," Final Technical Report, Contract F30602-88-C-0110, SRI International, Menlo Park, California (July).

Unger, J.H.W., R.H. Hardin, and R.J. Horan, 1973: "Auroral Clutter in UHF Radar," Technical Report, Contract Nos. DAHC60-69-C-0008 and F19628-73-C-0002, Bell Laboratories, Whippany, N. J.